High-precision figure correction of x-ray telescope optics using ion implantation

Brandon Chalifoux*[a], Edward Sung[a], Ralf K. Heilmann[b], Mark L. Schattenburg[b]
[a]Dept. of Mechanical Engineering, MIT, Cambridge, MA, USA 02139
[b]Space Nanotechnology Lab, MIT Kavli Institute, Cambridge, MA, USA 02139

*bchal@mit.edu; phone: (860) 377-1570; fax: (617) 452-2888; snl.mit.edu

ABSTRACT

Achieving both high resolution and large collection area in the next generation of x-ray telescopes requires highly accurate shaping of thin mirrors, which is not achievable with current technology. Ion implantation offers a promising method of modifying the shape of mirrors by imparting internal stresses in a substrate, which are a function of the ion species and dose. This technique has the potential for highly deterministic substrate shape correction using a rapid, low cost process. Wafers of silicon and glass (D-263 and BK-7) have been implanted with Si+ ions at 150 keV, and the changes in shape have been measured using a Shack-Hartmann metrology system. We show that a uniform dose over the surface repeatably changes the spherical curvature of the substrates, and we show correction of spherical curvature in wafers. Modeling based on experiments with spherical curvature correction shows that ion implantation could be used to eliminate higher-order shape errors, such as astigmatism and coma, by using a spatially-varying implant dose. We will report on progress in modelling and experimental tests to eliminate higher-order shape errors. In addition, the results of experiments to determine the thermal and temporal stability of implanted substrates will be reported.

Keywords: x-ray optics, telescope optics, shape correction, ion implantation, stress, roughness, stability

1. INTRODUCTION

The next generation of x-ray telescopes, in order to achieve sub-arcsecond resolution with large apertures, requires thin and lightweight optics with extremely precise figure, low mid-spatial frequency errors, and excellent surface roughness. In recent years, impressive strides have been made in the development of high resolution lightweight optics for x-ray telescopes, but sub-arcsecond resolution optics have not been demonstrated with current technology. Current methods of fabricating high-resolution thin optics involve replication of mandrels, either through deposition of nickel on the mandrel[1], or slumping of glass onto a mandrel[2]. Silicon is also used to fabricate high-resolution thin optics[3,4]. While these methods are currently capable of fabricating high-resolution thin optics, none have yet demonstrated sub-arcsecond resolution optics. Fine figure correction using ion implantation could push the current resolution limits beyond the arcsecond threshold. Combining ion implantation with glass slumping on air bearing mandrels[5] is particularly attractive because mid-spatial frequency errors are avoided; thus the slumped glass requires only figure correction.

Ion implantation, a process that has been used in the semiconductor industry for several decades, offers a promising method of precision shaping of thin substrates by causing sub-surface stresses that deform the substrate. During ion implantation, ions are accelerated to anywhere between 50 keV and >1 MeV, and directed toward a substrate. The ion cross-section is sufficiently small that it passes through the surface, and is slowed by electronic and nuclear forces within the substrate[6]. Implanted ions stop in a narrow range of depths, forming a near-Gaussian concentration profile. As noted by others[7,8,9], a repeatable sub-surface stress is imparted by the implantation process, although the mechanisms are not always known. The implanted ions cause damage to the substrate structure, impart energy into the substrate, and when stopped take up space in the substrate.

In this work, we have investigated the use of ion implantation for fine shape modification of thin substrates; in particular, we have studied the effect of implanting various ion species on the shape of silicon and Schott D-263T borosilicate glass wafers. Ion implantation is attractive because it is a low-cost process that can impose repeatable local stresses over the surface of a substrate. One key benefit over methods involving deposition of actuators or material on the substrate[10,11, 12] is that ion implantation does not cause its own errors that must be removed in addition to the figure errors of the

Optics for EUV, X-Ray, and Gamma-Ray Astronomy VI, edited by Stephen L. O'Dell, Giovanni Pareschi, Proc. of SPIE Vol. 8861, 88610T · © 2013 SPIE
CCC code: 0277-786X/13/$18 · doi: 10.1117/12.2023535

substrate. In addition, we are able to implant on both sides of a substrate since the surface is unaffected. This simplifies the substrate figure correction process. Aside from shape correction, two other important attributes of ion implantation are investigated: surface roughness and stress relaxation.

2. ION IMPLANTATION STRESS

Ions implanted into substrates impart sub-surface stress, which causes a measurable shape change. In order to modify substrate shapes in a predictable way, it is necessary to determine the imparted stress as a function of one or more variables. Similar to measuring stress arising from thin film deposition, if a substrate is implanted with a uniform dose distribution over its surface, the resulting shape change will be a change in spherical curvature. This change in spherical curvature follows Stoney's Equation[13]:

$$\sigma t_f = \frac{E h_s^2}{6(1-\nu)}\left(\frac{1}{R_1} - \frac{1}{R_0}\right), \quad (1)$$

where h_s is the substrate thickness, E is Young's modulus, ν is Poisson's ratio, R is the radius of curvature, and σt_f is the integrated stress. The integrated stress is used here because, unlike with a deposited film, there is no well-defined film thickness, t_f. The integrated stress of ion implantation can be directly compared to the integrated stress of a deposited film.

Previous researchers have found a strong – and monotonic over certain ranges – effect of dose on stress. Typically, this stress is found to be compressive, but some researchers have observed tensile stresses from high energy implants of light ions[14]. For the experiments in this work, the stress was measured as dose was varied and all other variables were held constant.

In these experiments, the wafer shapes were measured with a Shack-Hartmann metrology tool[15], using a low-stress optic mount[16]. The stress measurement is repeatable to $\pm 10^{-6}$ MPa-m. A total of 107 wafers were implanted with a uniform dose distribution and the shape measured before and after. A summary of the implanted wafers is shown in Table 1. All ion species were implanted at 150 keV, and the beam current limited to 60 uA to keep the wafer temperature below 150 °C. The doses ranged from 1.0 x 10^{14} ions/cm^2 to 2.0 x 10^{16} ions/cm^2. All implants were performed by CuttingEdge Ions, LLC. All wafers were 100 mm diameter, and the thickness ranged between 400 μm and 560 μm.

Table 1. Summary of implanted substrates

Substrate	Species	Number of samples
Silicon	Si+	36
Silicon	B+	5
BK-7	Si+	18
BK-7	Ar+	15
D-263T	Si+	24
D-263T	Al+	9
Total		107

2.1 Ion implantation of silicon wafers

Silicon implanted with Si+ results in a monotonic integrated stress-dose relationship over a large range of doses, shown in Figure 1. This stress is compressive. Beyond about 1 x 10^{16} ions/cm^2, the stress begins to fall off. This phenomenon has been observed previously. The monotonic range is useful for shape correction, which will be discussed later. In silicon, this compressive stress likely arises from lattice disorder or damage from the implant, as well as ion stuffing. There are a few outlying data points, which may be due to measurement error during early experiments. Silicon implanted with B+ showed similar behavior, but smaller in magnitude.

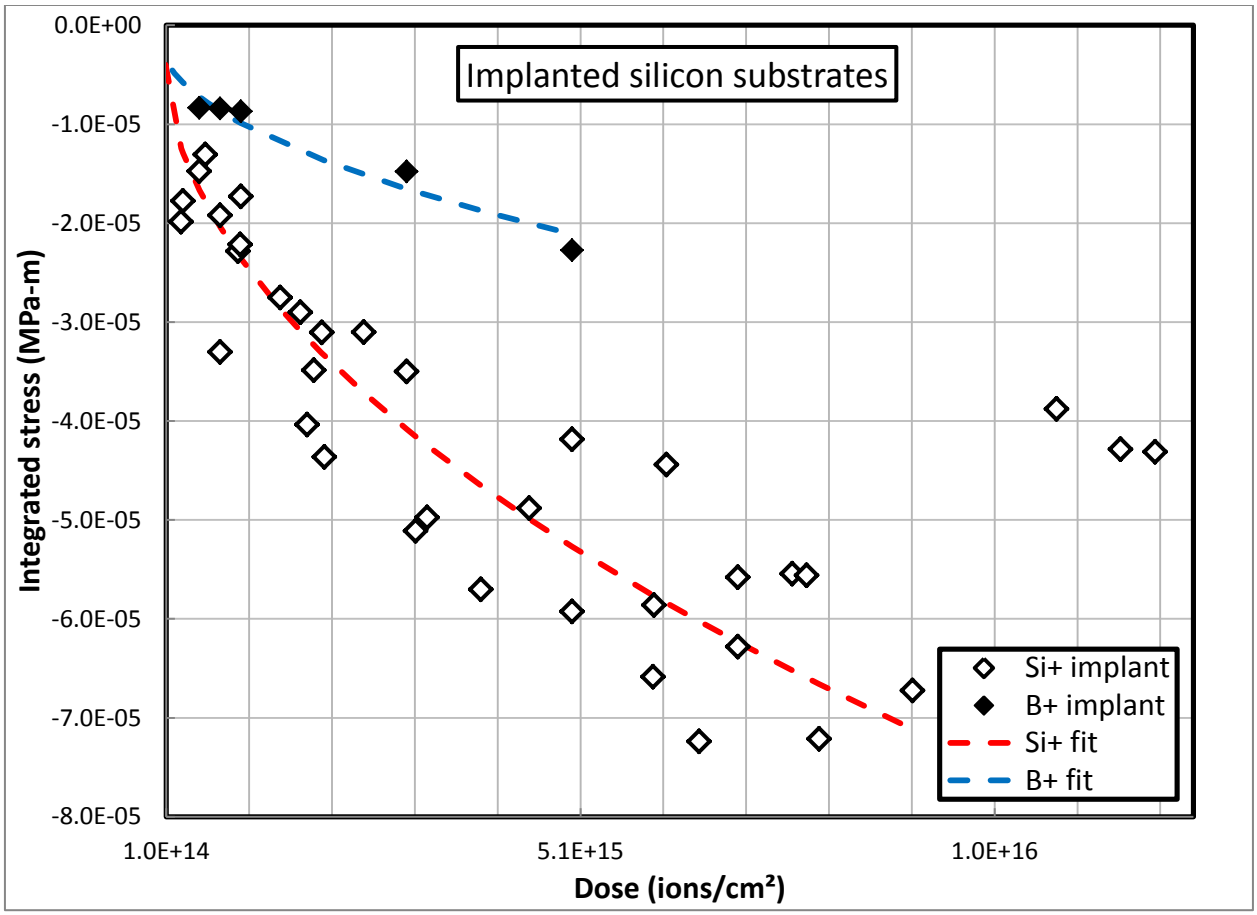

Figure 1. Integrated implant stress as a function of implant dose for Si+ and B+ implanted into silicon wafers. Ion energy is 150 keV, beam current is 60 μA. Each data point represents one wafer.

2.2 Ion implantation of glass wafers

The primary application of this work is to perform shape correction on slumped D-263 substrates. 16 wafers that had previously been slumped on air bearing mandrels[5] were implanted with Al+ and Si+. In addition, 17 unslumped wafers were implanted with Si+. Early experiments used BK-7 wafers due to their flatter shapes, which were initially easier to measure. The resulting integrated stress-dose relations, shown in Figures 2 and 3, are monotonic for small doses, and saturate at high doses. For both D-263 and BK-7, the magnitude of the stress is lower than that for silicon wafers, but large enough for fine shape correction, as will be discussed later. Results of BK-7 implanted with Ar+, show little promise for shape correction, but both BK-7 and D-263 implanted with Si+ show similar behavior to implanted silicon wafers.

The results of these experiments highlight a difference between the surfaces of the two chemically-similar glasses: BK-7 is ground and polished to size, while D-263 is made using a fusion process[17], and the surfaces are not mechanically polished. While Si+ implanted into BK-7 results in a compressive stress, Si+ implanted into D-263 results in a tensile stress, of similar magnitude. The compressive stress in BK-7 is expected based on the results with silicon wafers, but the tensile stress observed in D-263 is surprising. This tensile stress may be due to the thermal history of the D-263 glass. When D-263 is cooled from the melt, a temperature gradient near the surface during solidification causes compressive near-surface stresses. Slumping at a high temperature for a long time may relieve these surface stresses, but most of these samples were slumped just above the annealing point of the glass for relatively short times. There is no noticeable difference between the stress from the slumped and unslumped D-263 wafers, also suggesting that there has been little change to the glass structure during slumping. When the glass is implanted with high energy ions, the energy may cause some stress relief in this pre-stressed layer, countering any compressive effect from ion stuffing. This would appear as a tensile stress.

Additionally, two species with similar masses and volumes, Al+ and Si+, were chosen for implantation into D-263 to investigate whether chemical changes could be induced to increase the stress response. Aluminum could potentially cause chemical changes by replacing boron in B_2O_3, which may behave like ion exchange chemical hardening. However, the results from the two species are nearly identical, suggesting that the stress arises not from chemical changes, but primarily mechanical changes to the substrate.

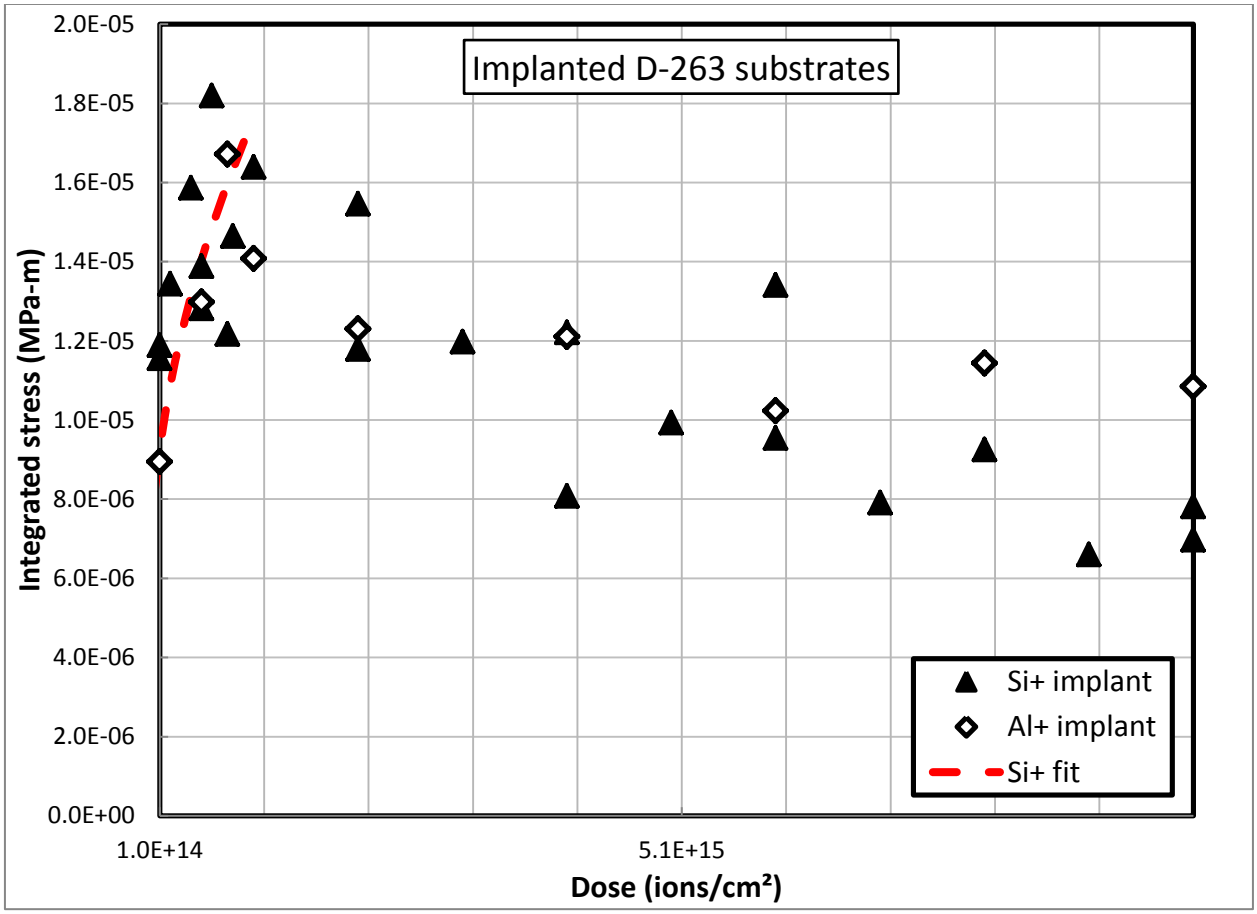

Figure 2. Integrated implant stress as a function of implant dose for Si+ and Al+ implanted into D-263 glass wafers. Ion energy is 150 keV, beam current is 60 μA. Each data point represents one wafer.

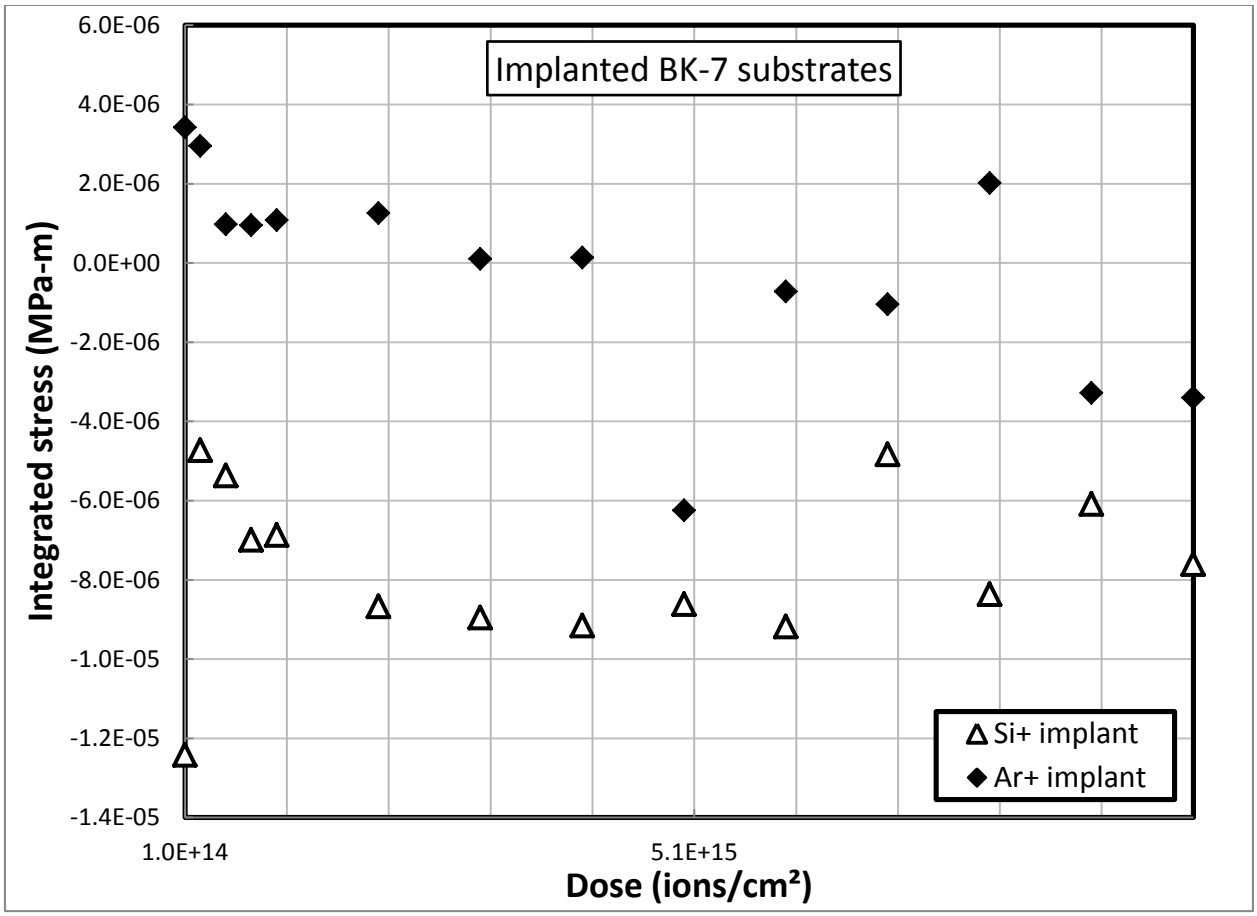

Figure 3. Integrated implant stress as a function of implant dose for Si+ and Ar+ implanted into BK-7 glass wafers. Ion energy is 150 keV, beam current is 60 μA. Each data point represents one wafer.

2.3 Stability of implanted wafers

It is critical that implanted thin telescope optics remain stable over many years in a reasonably well-controlled environment. In order to test for stability over reasonable experimental time scales, stability at elevated temperatures was tested. Stress relaxation of glasses in the solid glassy state follows Arrhenius' equation[18]:

$$\frac{K_1}{K_0} = e^{\frac{-E_a}{R}\left(\frac{1}{T_1}-\frac{1}{T_0}\right)}, \quad (2)$$

where K_0 and K_1 are the relaxation rates at temperatures T_0 and T_1, R is the universal gas constant, and E_a is the activation energy associated with the relaxation process. E_a is unknown for implanted substrates, but may be similar to relaxation tempered glass, where E_a has been measured to be 300-500 kJ/mol[19]. Choosing T_0 = 293 K, T_1 = 343 K, and E_a = 300 kJ/mol, $K_1/K_2 > 10^8$. Thus, exposure to 70 °C for 4 hours corresponds to > 60,000 years, and is sufficient to establish long-term stability of the implanted glass.

This experiment involved measuring implanted wafers, then exposing them to an elevated temperature for 4 hours, and measuring them again. The wafers were then exposed to progressively higher temperatures for 4 hours at a time, and measured after each interval. The results are shown in Figure 4, calculated as a change in integrated stress. The repeatability of the stress measurement is near $\pm 10^{-6}$ MPa-m, which represents the entire range of this plot. Six slumped D-263 wafers implanted with Si+ and Al+, and one silicon wafer implanted with Si+, were tested. No wafer exhibited any discernible stress relief larger than the repeatability of the metrology tool.

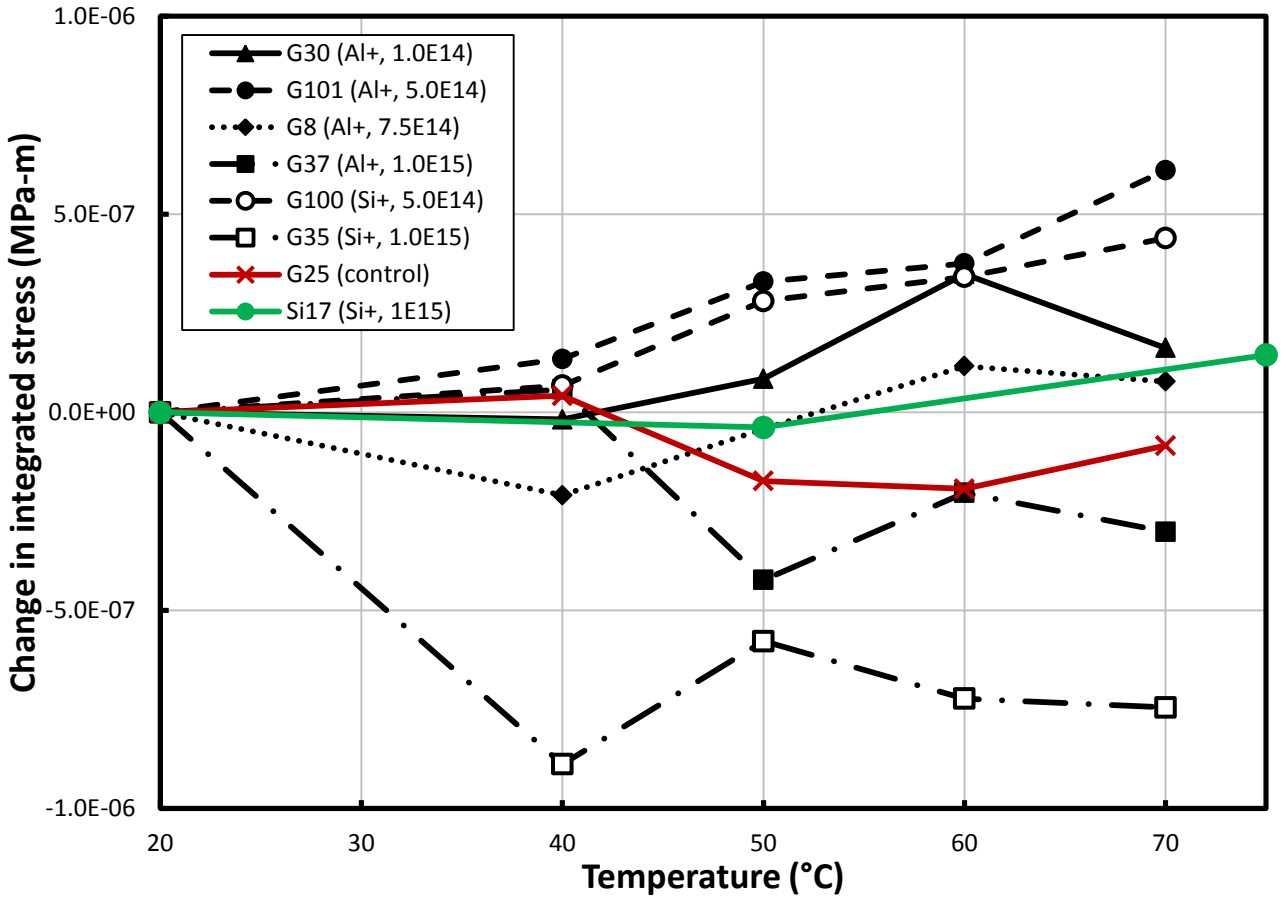

Figure 4. Change in integrated stress resulting from exposure to elevated temperatures. These changes are within the repeatability of the Shack-Hartmann metrology tool, $\pm 10^{-6}$ MPa-m.

2.4 Effects on surface roughness

It is critical that the surface roughness of the mirror substrates remain low to maintain a high x-ray reflectivity. Firing high energy ions into the mirror substrates could potentially cause some roughening. Other researchers have noted both increases and decreases in surface roughness due to ion implantation in fused silica[20]. To determine the effect on surface roughness, x-ray reflectivity curves were measured before and after ion implantation for D-263, and silicon. A 9 kW rotating anode, copper-Kα x-ray source with a Rigaku SmartLab instrument was used to measure the reflectivity curves. Two silicon and two D-263 wafers were measured, and results from both were nearly identical. One reflectivity curve for each substrate is shown in Figures 5 and 6. The samples shown here were implanted with Si+ at 150 keV and 60 μA, as with all other samples in this work. The dose for the silicon sample was $2x10^{15}$ ions/cm^2, and the dose for the D-263 sample was $2x10^{14}$ ions/cm^2. It is difficult to accurately fit a model to the reflectivity curves, due to minor surface contamination and thin surface films, but the change in reflectivity observed in silicon is consistent with significantly less than a 1Å change in roughness. This is clear when the measured x-ray reflectivity data are compared to two modeled reflectivity curves with a 1Å difference in surface roughness.

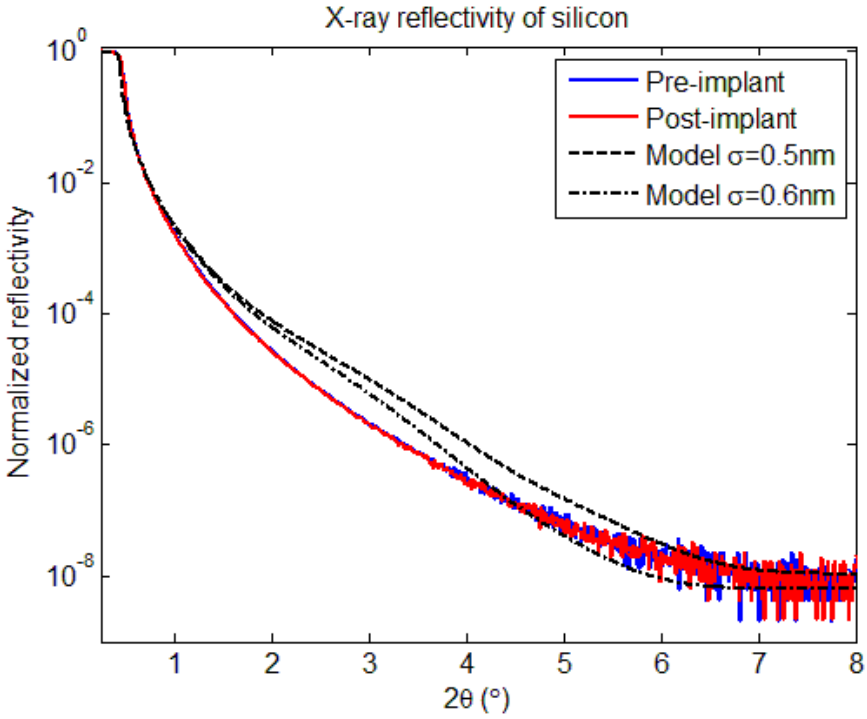

Figure 5. X-ray reflectivity for implanted silicon, and representative reflectivity models. This sample is representative of the silicon substrates measured. This sample was implanted with Si+ at a dose of $2x10^{15}$ ions/cm^2, ion energy of 150 keV, and a beam current of 60 μA. The change in roughness is negligible.

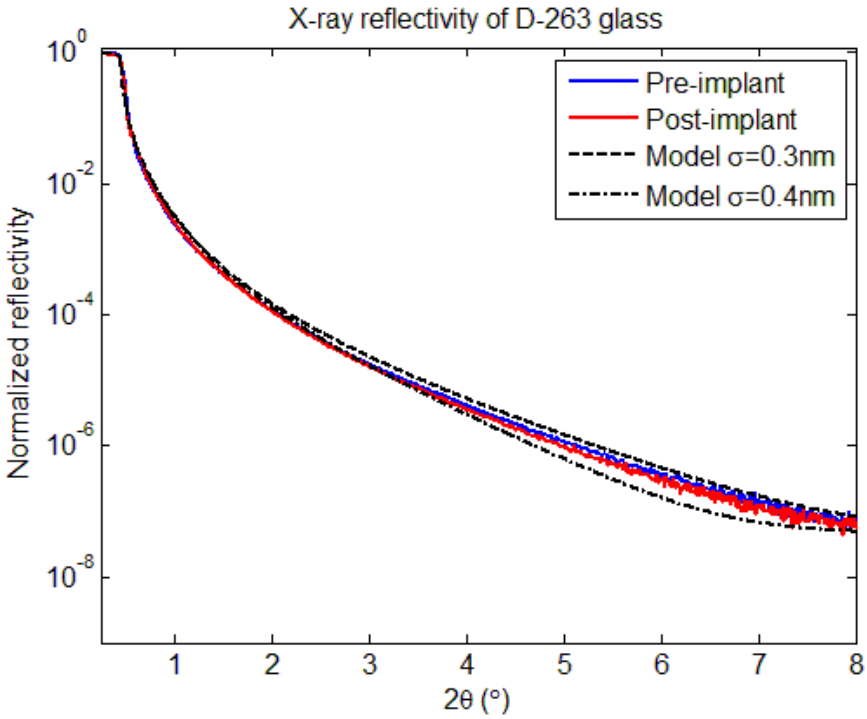

Figure 6. X-ray reflectivity for implanted D-263 glass, and representative reflectivity models. This sample is representative of the D-263 samples measured. This sample was implanted with Si+ at a dose of $2x10^{14}$ ions/cm^2, ion energy of 150 keV, and a beam current of 60 μA. The change in roughness is much less than 1 Å.

3. SHAPE CORRECTION

The primary goal of this work is to correct figure errors in x-ray telescope mirror substrates. Understanding the nature of stress resulting from ion implantation is a valuable step, but demonstrating an ability to actually correct figure errors is of critical importance. While working with parabolic or hyperbolic grazing-incidence optics is ideal, there are two short-term barriers that restrict this work to flat wafers: 1) commercial processes, including ion implantation, are only equipped to handle flat wafers; and 2) in order to correct most figure errors, implanting a non-uniform dose distribution is required, which commercial ion implanters are not capable of. Due to these barriers, this work focuses on shape correction of flat silicon wafers. Silicon wafers were chosen over glass because they are easier to work with for commercial implanters, as well as in other fabrication equipment. We show experimental results demonstrating correction of both spherical curvature and astigmatism. In addition, we show modeled results of shape correction in thin cylindrical glass optics, and show that substantial correction is feasible with ion implantation.

3.1 Correcting spherical curvature

Correcting spherical curvature of a flat wafer is relatively simple, as this only requires a uniform dose distribution, which is exactly what commercial implanters are set up to do. With some implant data for Si+ implanted into silicon, we predicted the dose required to remove the spherical curvature. A total of 15 wafers were implanted with the intention of removing spherical curvature. The median reduction in spherical curvature was 5x, but with a wide range from 1.4x to 125x. Spherical curvature is measured as the P-V of the spherical component of the shape, which is inversely proportional to the radius of curvature. A typical example is shown in Figure 7, where the spherical curvature has been substantially reduced.

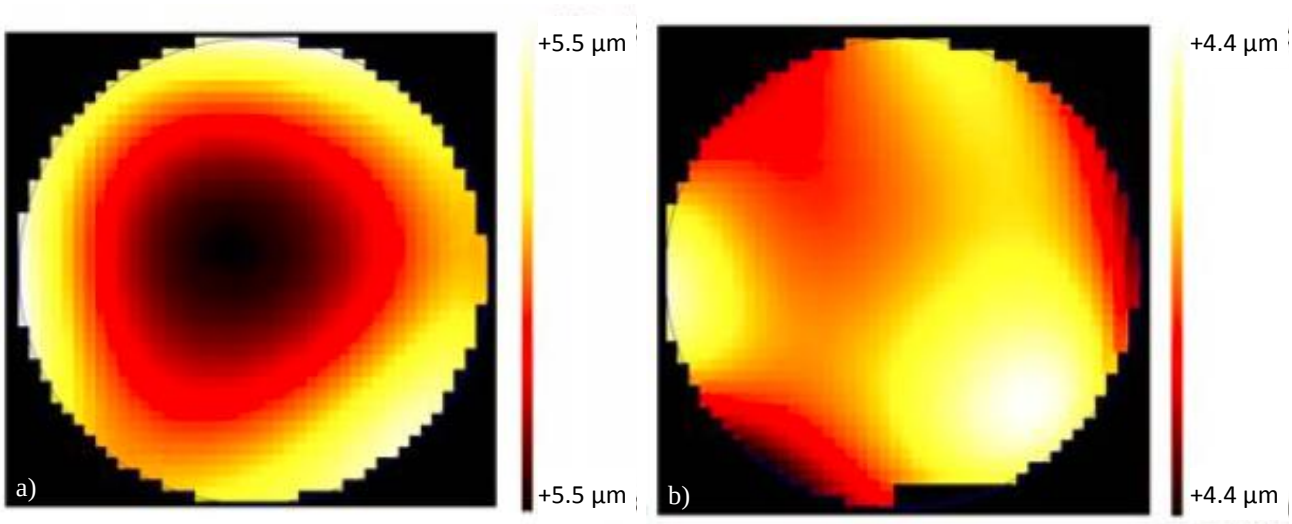

Figure 7. Example of deterministic spherical curvature correction, where dose was predicted before implant. (a) A sample prior to implant, which had a spherical curvature of 9 µm; (b) the same sample after a single implant, where the spherical curvature is -0.7 µm. The total reduction here was over 10x. As expected, no other figure errors were affected.

3.2 Correcting higher-order errors

Higher-order figure errors, such as astigmatism or coma, are more challenging to remove because they require a non-uniform dose distribution. Since commercial implanters are only capable of applying a uniform dose distribution (and therefore uniform stress distribution), masking was required to achieve a non-uniform dose distribution. In addition, a model used to calculate the required dose distribution was built. The first attempt to correct astigmatism was successful and provides some validation for the model.

The first challenge was to develop a model to calculate the stress distribution required to impart a given shape change. To solve this inverse problem, a commercial finite element package, ADINA, was used in conjunction with Matlab to impose various stress fields on a wafer and determine the resulting deformation. A spectral method using Zernike

polynomials to describe both the imposed stress fields and the deformed shapes was chosen to solve this problem with minimal computational resources; this method is illustrated in Figures 8 and 9, and described below.

The first step is to build a library of deformations resulting from various applied stress fields, as shown in Figure 8. This is similar to performing system identification by perturbing the system with sinusoidal inputs, except here, we choose to apply stress fields described by a single Zernike polynomial. We then decompose the resulting deformation into (often many) Zernike polynomials, and store the vector of coefficients in our library. This is repeated for numerous stress fields and their resulting deformations.

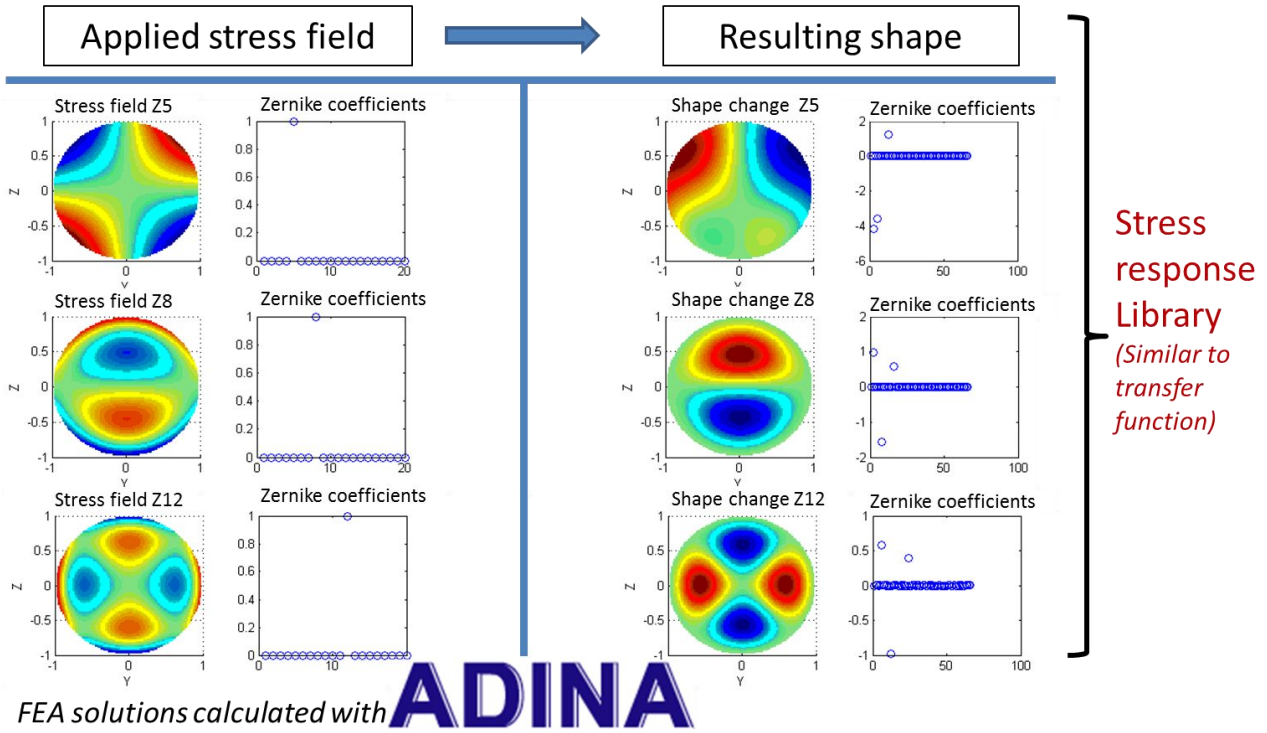

Figure 8. Stress response library for modal decomposition method of calculating ion implantation stress field to correct figure error.

Once the library is built, and we have a desired deformation composed of a set of Zernike polynomials, we can find a linear combination of stress fields that give a total deformation that best matches the desired deformation, in a least squares sense; this step is shown in figure 9. The result can then be checked by applying this best-fit stress field ADINA. The stress field can then be converted to a dose distribution.

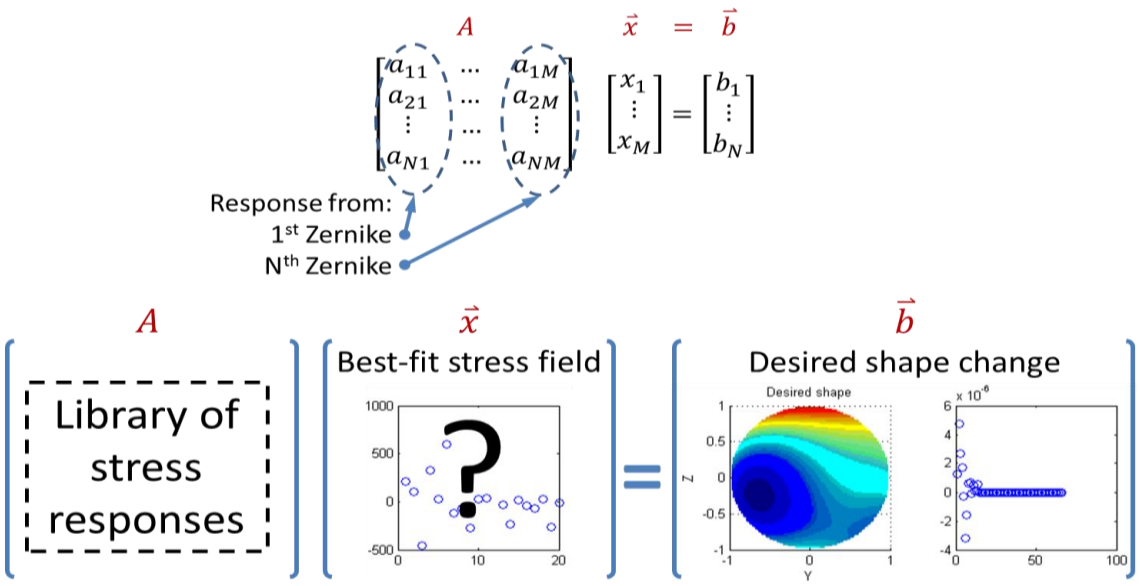

Figure 9. Finding the stress field that results in a shape change closest to the desired shape change, using a least-squares approach.

To demonstrate correction of higher-order figure errors, we set out to correct astigmatism in a silicon wafer. Using the modal decomposition model, a dose distribution was calculated to correct astigmatism, and used to generate a chrome photomask. The photomask is composed of a grid of squares of variable size; when this pattern is transferred to photoresist on the wafer, the photoresist blocks implanted ions inside the squares and allows ions to be implanted into the substrate outside the squares. The mask and photoresist are shown in Figure 10. Photoresist was applied to both sides of a wafer, aligned to the mask (both translation and rotation), exposed and developed. The masked wafer was then implanted with a dose of 3.9 x 10^{13} ions/cm^2 of Si+ on both sides. After cleaning, the wafer can then be measured. Figure 11 shows the shape change. The P-V of the astigmatism before implant was 5.2 μm, so the dose was clearly far too low. It was later determined that this was due to a labeling error. It is encouraging, however, that the change in shape is almost entirely astigmatism, providing some validation for the model.

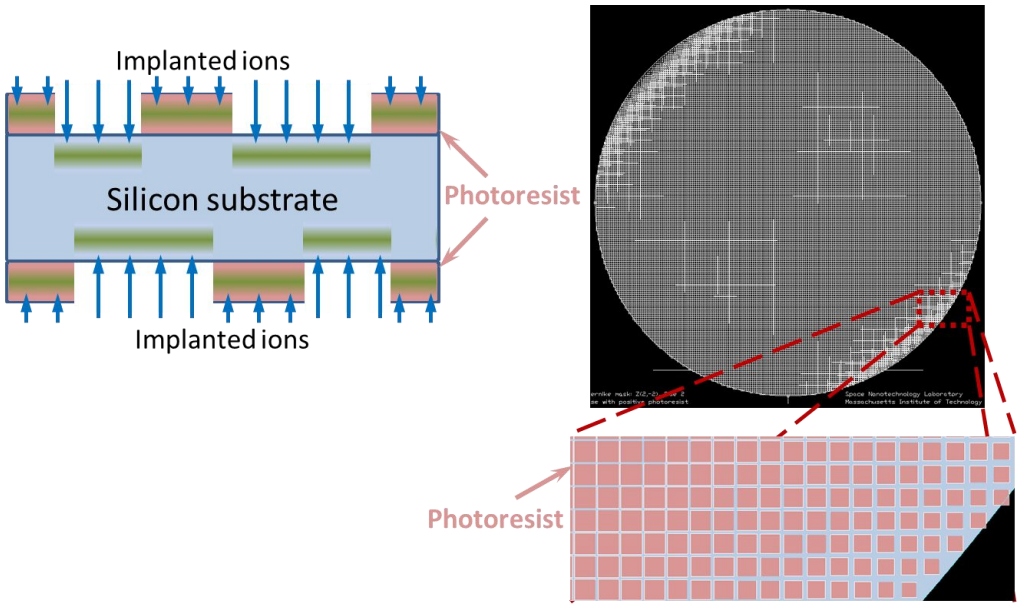

Figure 10. Method of using photoresist to cause a non-uniform dose distribution in silicon wafers. Photoresist is applied as a mask to both sides of a wafer, and the wafer is implanted with a uniform dose.

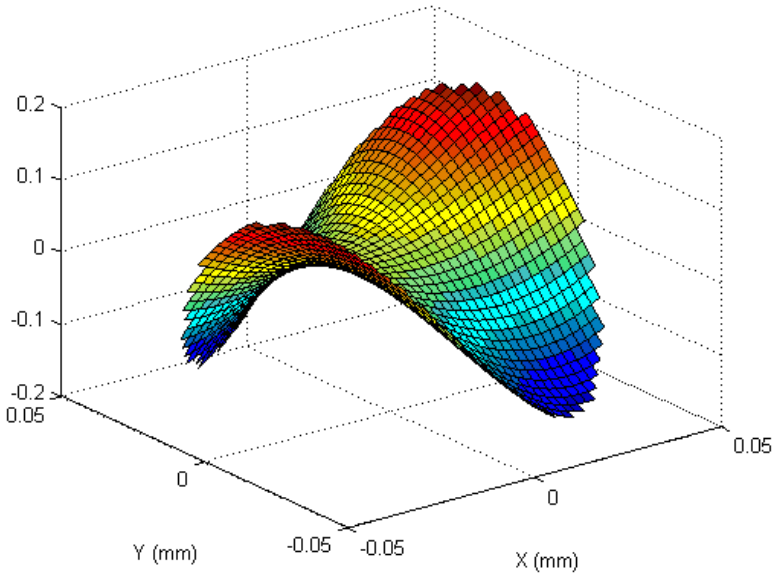

Figure 11. Experimental result showing change in astigmatism, while all other figure errors are unaffected.

3.3 Correcting Wolter type I optics

Wolter type I substrates are significantly more challenging to correct than flat substrates, for numerous reasons. First, commercial ion implanters are not set up to handle non-flat substrates. Second, depositing and exposing a masking layer on a near-cylindrical thin optic is impossible with commercial equipment. In addition, since commercial ion implanters are only capable of randomly-scanning the ion beam, it will be necessary to build an implanter with a custom substrate mount, and with a raster-scanning ion beam.

More fundamental to all methods of adjusting grazing-incidence optics, the stiffness in the axial direction is quite different than in the azimuthal direction. It is critical to know how much shape correction ion implantation is expected to be able to provide for Wolter optics. A model similar to the flat wafer model of Section 3.2 was built. Instead of using Zernike polynomials, which are each orthogonal to each other over a unit circle, Legendre polynomials and cylindrical coordinates were used. The rest of the process is identical to Section 3.2. In this model, 200mm long x 130mm wide x 0.4mm thick glass substrates with 500mm and 1000mm radii of curvature was used. A purely cylindrical optic was used because the effect of a parabolic or hyperbolic prescription is expected to be of lower order than the cylindrical curvature.

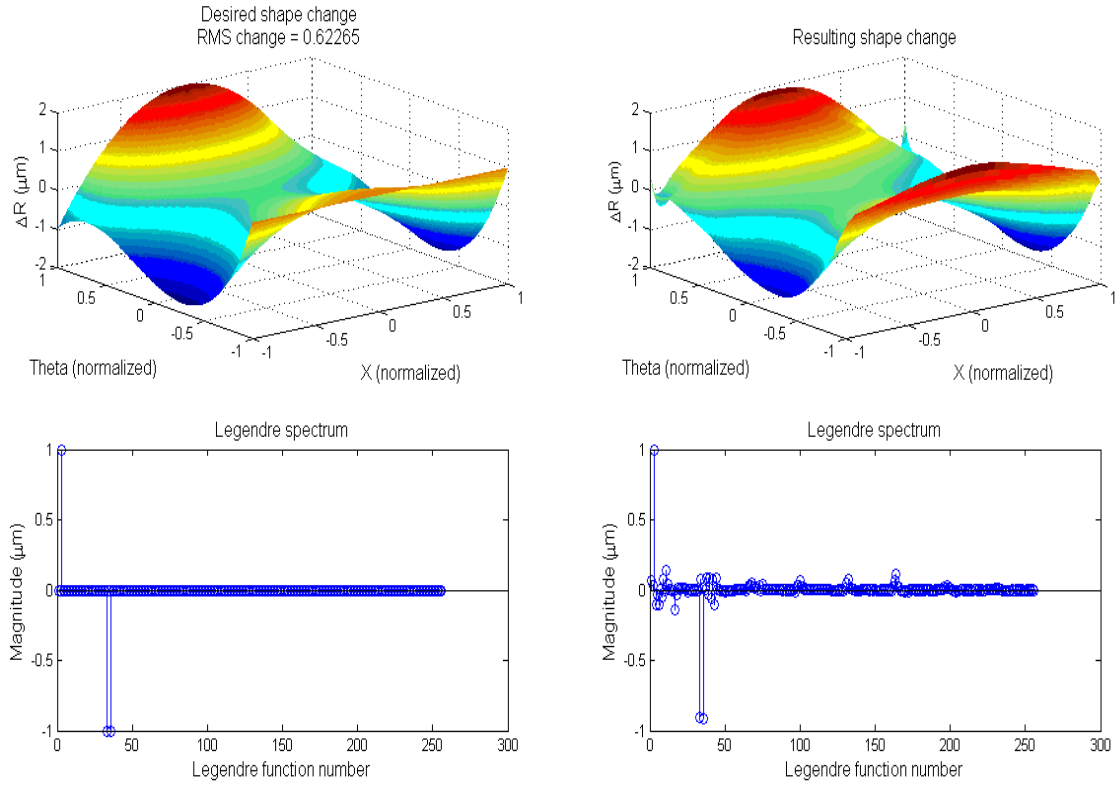

Figure 12. Preliminary numerical results for shape correction of segmented thin Wolter I optics using ion implantation and the modal decomposition method.

Results from this model are encouraging, but more work is necessary. While figure correction of low-order errors is achievable with very low integrated stress (of order 10^{-7} MPa-m), the RMS slope error in the axial direction does not significantly improve using this modal decomposition method. An influence function approach taken by Harvard-SAO[21] shows much more promising results, including a reduction of HPD by a factor of 5 to 10. The principle of shape correction with ion implantation is identical to that of the PZT actuators used in that study. It is possible that while using Zernike polynomials for circular flats is a useful approach, using Legendre polynomials for near-cylindrical optics is not a useful approach. Adapting the Harvard-SAO approach for ion implantation could show improved results, since ion implantation can have a variable beam size, potentially eliminating excited spatial frequencies from a fixed actuator spacing.

4. CONCLUSIONS AND FUTURE WORK

We have shown that ion implantation has potential to be the ideal process for figure correction of thin optics for x-ray telescope optics. Repeatable sub-surface stress can be rapidly applied in any pattern to both sides of an optic, allowing a wide range of correctable figure errors. We have shown experimentally that both spherical curvature and astigmatism can be corrected in silicon wafers. There is no reason this could not be applied to any arbitrary figure error, provided the spatial frequency is not too high.

Using thermal stability as a proxy for temporal stability, we have shown that implanted silicon and D-263 glass substrates experience no discernible stress relaxation. In addition, using x-ray reflectivity, we have shown that ion implantation has minimal effect on the surface roughness of both silicon and glass substrates.

Modeling, which has been validated for flat wafers, suggests that Wolter I segmented optics are also correctable. Unlike with flat wafers, correcting cylindrical optics cannot be achieved with commercial equipment. Thus, a custom ion implanter that can accommodate non-flat optics and that can perform raster-scanning of the ion beam must be built. Further work on modeling, as well as understanding the nature of the stress resulting from ion implantation, will also be necessary for this work.

REFERENCES

[1] S. Romaine, S. Basso, R. J. Bruni, W. Burkert, O. Citterio, G. Conti, D. Engelhaupt, M. J. Freyberg, M. Ghigo, P. Gorenstein, M. Gubarev, G. Hartner, F. Mazzoleni, S. O'Dell, G. Pareschi, B. D. Ramsey, C. Speegle, D. Spiga, "Development of a prototype nickel optic for the Constellation-X hard x-ray telescope: IV," Proc. SPIE 6266 (2006).

[2] W.W. Zhang, M.P. Biskach, P.N. Blake, K.W. Chan, T.C. Evans, M.L. Hong, W.D. Jones, L.D. Kolos, J.M. Mazzarella, R.S. McClelland, S.L. O'Dell, T.T. Saha, and M.V. Sharpe, "Lightweight and high angular resolution x-ray optics for astronomical missions," Proc. SPIE 8147 (2011).

[3] W. W. Zhang, M. P. Biskach, P. N. Blake, K.-W. Chan, J. A. Gaskin , M. L. Hong,W. D. Jones, L. D. Kolos, J. R. Mazzarella, R. S. McClelland, S. L. O'Dell, T. T. Saha, and M. V. Sharpe, "Next-generation astronomical x-ray optics: high angular resolution, light weight, and low production cost," Proc. SPIE 8443 (2012).

[4] Wallace, K., Bavdaz, M., Gondoin, P., Collon, M. J., Günther, R., Ackermann, M., Beijersbergen, M. W., Olde Riekerink, M., Blom, M., Lansdorp, B., & de Vreede, L., "Silicon-pore optics development", SPIE 7437 (2009).

[5] E. Sung, B. Chalifoux, M. L. Schattenburg, R.K. Heilmann, "Non-touch thermal air-bearing shaping of x-ray telescope optics," SPIE 8861 (2013).

[6] Wolf, S. and Tauber, R. N., [Silicon Processing for the VLSI Era, Vol. 1: Process Technology], Lattice Press, 283-308 (1986).

[7] M. Itoh and M. Hori, "An ultralow stress tungsten absorber for xray masks," J. Vac. Sci. Technol. B, 9, 165 (1991).

[8] A. Misra, S. Fayeulle, H. Kung, T.E. Mitchell, M. Nastasi, "Residual stresses and ion implantation effects in Cr thin films," Nuclear Instruments and Methods in Physics Research B, 148, 211-215 (1999).

[9] P.J. Burnett and T.F. Page, "An investigation of ion implantation-induced near-surface stresses and their effects in sapphire and glass," J. Mat. Sci. 20, 4624-4646 (1985).

[10] V. Cotroneo, W.N. Davis, V. Marquez, P.B. Reid, D.A. Schwartz, R.L. Johnson-Wilke, S.E. Trolier-McKinstry, R.H.T. Wilke, "Adjustable grazing incidence x-ray optics based on thin PZT films," Proc. SPIE 8503 (2012).

[11] K. Kilaru, B.D. Ramsey, M.V. Gubarev, D.A. Gregory, "Differential deposition technique for figure corrections in grazing-incidence x-ray optics," Optical Eng. 50(10) (2011).

[12] M.P. Ulmer, M.E. Graham, S. Vaynman, J. Cao, P.Z. Takacs, "Deformable mirrors for x-ray astronomy and beyond," SPIE 8076 (2011).

[13] G.G. Stoney, "The tension of metallic films deposited by electrolysis," Proc. Royal Society of London, A, 82 (553) 172-175 (1909).

[14] E. Snoeks, T. Weber, A. Cacciato, A. Polman, "MeV ion irradiation-induced creation and relaxation of mechanical stress in silica," J. Appl. Phys. 78, 4723 (1995).

[15] C.R. Forest, C.R. Canizares, D.R. Neal, M. McGuirk, M.L. Schattenburg, "Metrology of thin transparent optics using Shack-Hartmann wavefront sensing," Opt. Eng. 43(3) 742-753 (2004).

[16] M. Akilian, C.R. Forest, A.H. Slocum, D.L. Trumper, M.L. Schattenburg, "Thin optic constraint," Precision Eng. 31, 130-138 (2007).

[17] A. Ellison and I.A. Cornejo, "Glass substrates for liquid crystal displays," Int. J. Appl. Glass Sci. 1(1) 87-103 (2010).

[18] S. Rekhson, "Models of relaxation in glass," J. Non-Crystalline Solids, 95 & 96, 131-148 (1987).

[19] O.S. Narayanaswamy, "Stress and structural relaxation in tempering glass," J. Amer. Ceramic Soc., 61 (3-4), 146-152 (1978).

[20] K. Oyoshi, S. Hishita, K. Wada, S. Suehara, T. Aizawa, "Roughness study of ion-irradiated silica glass surface," Appl. Surface Sci., 100/101, 374-377 (1996).

[21] T.L. Aldcroft, D.A. Schwartz, P.B. Reid, V. Cotroneo, W.N. Davis, "Simulating correction of adjustable optics for an x-ray telescope," Proc. SPIE 8503 (2012).